PAPR Minimization via Constructive Interference Precoding For Multi-User MISO-OFDM System

Yuanyuan Qin, Xuewen Liao, Ang Li, *Member, IEEE*, and Christos Masouros, *Senior Member, IEEE*

***Abstract*—This paper proposes a method exploiting constructive interference (CI) effect to reduce the high peak-to-average power ratio (PAPR), while keeping the total transmission power as low as possible. An optimization problem that jointly performs power minimization and PAPR reduction is formulated, which is however difficult to solve directly due to the non-convex PAPR constraint. To obtain a feasible solution in low complexity, by using the vectorization method and introducing a regularization factor, we relax the PAPR constraint and the original optimization problem is transformed into a convex problem that can be solved with an improved fast iterative shrinkage-thresholding algorithm (FISTA). Numerical results are presented to validate the enhanced performance of the proposed method in terms of transmission power and PAPR compared with state-of-the-art PAPR minimization techniques.**

***Index Terms*—MISO-OFDM, PAPR, symbol-level precoding, constructive interference (CI).**

I. Introduction

MIMO and OFDM are effective techniques in fulfilling the constantly increasing throughput requirements of wireless communication systems. In MIMO-OFDM systems, the transmit signals fluctuate dynamically and usually have high peak-to-average-power ratio (PAPR), which in practical wireless communication systems due to the nonlinear effect and imperfection of power amplifiers (PAs) and digital-to-analog converters (DACs). Therefore, it is of great practical significance to suppress PAPR before OFDM signals pass through DACs and PAs.

To alleviate the nonlinear distortions from practical DACs and PAs, a variety of PAPR-reduction techniques for single-antenna OFDM systems have been proposed [1]–[3], which can be divided into three categories: signal processing based techniques [1], probabilistic techniques [2] and coding techniques [3]. However, these approaches are not very effective when extending to MIMO system, mainly because MIMO system requires the management of multi-user interference (MUI). In this case, a desirable solution is to design an appropriate precoding scheme to manipulate the transmitted signals to suppress PAPR as well as MUI. Based on this idea, [4] first proposes a precoding method called Joint Precoding, Modulation and PAPR Reduction (PMP) algorithm that exploits the degree-of-freedom (DoF) offered by the large number of antennas at the base station (BS) to perform MUI elimination, OFDM modulation and PAPR reduction at the same time. This scheme performs well when the number of transmit antennas is large, but as DoF goes down, its PAPR reduction ability becomes less effective.

Recently, symbol-level precoding (SLP) has been studied widely [5], [6]. Different from conventional block-level precoding, SLP is a novel strategy using the knowledge of both the channel state information (CSI) and data information, which allows to handle MUI in a more effective way. With the exploitation of constructive interference (CI) effect, some schemes have studied PAPR suppression based on CI precoding [7]–[11]. For example, [7] applys the idea of CI to constant-envelope precodig (CEP) that directly enforces the amplitude of the transmit signals to be constant for a PSK-modulated massive MIMO system and proposes two different CEP approaches, which redefines the optimization region for CEP and transforms the MUI as a source of additional energy to increase the SINR at the receiver. [12] proposes a low-complexity manifold-based algorithm to solve the CI-based CEP optimization. By viewing the feasible region of the CE optimization as an oblique manifold, it can efficiently find a near-optimal solution using the Riemannnian conjugate gradient algorithm and thus reduces the computational complexity. While CEP allows the lowest PAPR value, the strict CE constraints introduce significant signal distortions for small-and medium-scale MIMO systems. To address this issue, [8] and [9] perform spatial peak-to-average power ratio (SPAPR) minimization subject to the quality of service (QoS) constraints with per-antenna power constraint. [10] minimizes the PAPR of the transmitted waveform in both space and time domain by proposing a spatio-temporal SLP algorithm based on the equivalent space-time channel. [11] limits the power peaks by reducing the imbalance between the instantaneous transmit power on each transmit antenna and improves robustness of the transmit signals to non-linear distortion. However, the above CI-based PAPR reduction methods fail to exhibit desirable tradeoff between PAPR suppression and communication performance, while still incurring significant computational costs due to the complication of the formulated optimization problems.

In this letter, we design a precoding scheme based on CI for PAPR reduction in a MIMO-OFDM system, which effectively reduces PAPR while offers a promising communication performance in low complexity. Specifically, a power minimization (PM) problem subject to the PAPR and CI constraints is constructed, which is shown to be non-convex. By using vectorization and regularization method, we relax the PAPR constraint to transform the original problem into a convex one, and further design a low-complexity iterative algorithm based on the fast iterative shrinkage-thresholding algorithm (FISTA) [13]. Simulation results exhibit superior performance of our scheme over the existing schemes in terms of total transmission power, PAPR performance and computational complexity.

Notations: In this paper, bold lowercase and uppercase letters denote vectors and matrices respectively. $(\cdot)^T, (\cdot)^H, (\cdot)^*, \sigma_{max}(\cdot)$ represent transpose, conjugate transpose, conjugate and the largest singular value respectively. $vec(\cdot)$ arranges a matrix into a column vector and $diag(\cdot)$ transforms a column vector into a diagonal matrix. ℓ_2-norm, ℓ_∞-norm of a vector and Frobenius norm of a matrix are denoted by $\|\cdot\|_2, \|\cdot\|_\infty$ and $\|\cdot\|_F$ respectively. $\mathbf{I}_M$ denotes a $M \times M$ identity matrix, $\succeq$ and $\preceq$ are used as generalized inequalities for two vectors, while $\otimes$, $\bullet$ and $\bigtriangledown$ denote the Kronecker Product, the dot product operation and the gradient operator respectively.

II. System Model and Preliminaries

A. System Model

Consider a MISO-OFDM system, where the BS is equipped with M_t transmit antennas to serve a total number of $K \leq M_t$ single-antenna users. At the BS, bit streams are modulated into M-PSK symbols, and OFDM modulation is used to combat multipath fading, where the number of OFDM subcarriers is N. The modulated data matrix is denoted by $\mathbf{S} = [\hat{\mathbf{s}}_1, \hat{\mathbf{s}}_2, \cdots, \hat{\mathbf{s}}_K]^T$, where user k's data symbols $\hat{\mathbf{s}}_k \in \mathbb{C}^{N\times 1}$ are firstly precoded by a precoding matrix and then sent to each antenna for OFDM modulation to obtain the time-domain samples. The transmit signal matrix $\mathbf{Z} \in \mathbb{C}^{M_t \times N}$ on all subcarriers can be given by

$$\mathbf{Z} = \left(\mathbf{F}_N^H \mathbf{X}^T\right)^T = \mathbf{X}\mathbf{F}_N^* \tag{1}$$

where $\mathbf{X} \in \mathbb{C}^{M_t \times N}$ is the precoded signal, $\mathbf{F}_N \in \mathbb{C}^{N\times N}$ is the fast Fourier transform (FFT) matrix. Expressing the channel matrix at each frequency point as $\mathbf{H}_n = [\mathbf{h}_1^T, \mathbf{h}_2^T, \cdots, \mathbf{h}_K^T]^T \in \mathbb{C}^{K\times M_t}$, $n = 1, 2, \cdots N$, the received signal $\mathbf{Y} = [\hat{\mathbf{y}}_1, \hat{\mathbf{y}}_2, \cdots, \hat{\mathbf{y}}_K]^T \in \mathbb{C}^{K\times N}$ can be written as:

$$\mathbf{y}_n = \mathbf{H}_n \mathbf{x}_n + \mathbf{n}_0 \tag{2}$$

where $\mathbf{x}_n \in \mathbb{C}^{M_t \times 1}$ is the n-th column of $\mathbf{X}$, $\mathbf{y}_n \in \mathbb{C}^{K\times 1}$ is the n-th column of $\mathbf{Y}$, $\mathbf{n}_0 \in \mathbb{C}^{K\times 1}$ is the Additive White Gaussian Noise on the n-th subcarrier.

At each user side, FFT operation is performed on the received signal $\hat{\mathbf{y}}_k$ for demodulation to obtain the required signal $\mathbf{R} = [\hat{\mathbf{r}}_1, \hat{\mathbf{r}}_2, \cdots, \hat{\mathbf{r}}_K]^T \in \mathbb{C}^{K\times N}$, with each $\hat{\mathbf{r}}_k$ given by

$$\hat{\mathbf{r}}_k = \left(\mathbf{F}_N \hat{\mathbf{y}}_k^T\right)^T = \hat{\mathbf{y}}_k \mathbf{F}_N^T \tag{3}$$

B. Peak-to-average Power Ratio (PAPR)

The PAPR at the m-th antenna can be expressed as:

$$PAPR_m = \frac{\max\limits_{1\leq n\leq N}\{|z_n|^2\}}{\mathbb{E}[|z_n|^2]} = \frac{\|\mathbf{z}\|_\infty^2}{\|\mathbf{z}\|_2^2/N} = N\frac{\|\mathbf{z}\|_\infty^2}{\|\mathbf{z}\|_2^2} \tag{4}$$

where $z_n, n = 1, 2, \cdots, N$ stands for an OFDM symbol of the m-th antenna.

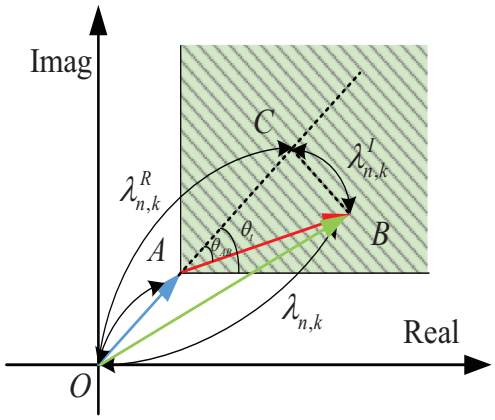

Fig. 1: An illustration for the beneficial interference region and mathematical CI condition

C. Constructive Interference Precoding

CI precoding is a new technique to make use of interference by proposing the concept of beneficial interference region. Taking QPSK modulation as an example, the beneficial interference region and the corresponding mathematical formulation of CI is shown in Fig. 1 above [6].

As shown in Fig. 1, $\overrightarrow{OB} = \mathbf{H}_n\mathbf{x}_n$ represents the received noiseless signal of the n-th subcarrier, and $\overrightarrow{OA} = ts_{n,k}$ is a scaled version of the original data symbols, where the parameter t can be viewed as a measurement of the received SINR, i.e., $t = \sqrt{\Gamma_{n,k}\sigma^2}$, where σ^2 is the noise variance, $\Gamma_{n,k}$ is the received SINR threshold of the k-th user at the n-th subcarrier and the matrix $\mathbf{\Gamma} \in \mathbb{C}^{K\times N}$ represents the SINR threshold of all the users on each subcarrier. We further introduce a parameter $\boldsymbol{\lambda}_n \in \mathbb{C}^{K\times 1}$, which is termed as a phase rotation factor to represent the impact of MUI to make $\overrightarrow{OB} = \mathbf{H}_n\mathbf{x}_n = \boldsymbol{\lambda}_n \bullet \mathbf{s}_n$, where $\mathbf{s}_n \in \mathbb{C}^{K\times 1}$ is the n-th column of the original data matrix $\mathbf{S}$ and $\boldsymbol{\lambda}_n$ is the n-th column of the matrix $\mathbf{\Lambda}$. To realize CI effect, according to the geometric relationship, the noiseless received signals should lie in the green shaded constructive region, which is mathematically equivalent to: $\theta_{AB} \leq \theta_t$, where $\theta = \frac{\pi}{M}$ for M-PSK.

With some further transformations, the CI condition under M-PSK modulation can be expressed as [5]:

$$\left(\lambda_{n,k}^R - \sqrt{\Gamma_{n,k}\sigma^2}\right)\tan\theta_t \geq \left|\lambda_{n,k}^I\right| \quad \forall n = 1, \cdots, N, \quad k = 1, \cdots, K \tag{5}$$

where $\lambda_{n,k}$ is the k-th element of $\boldsymbol{\lambda}_n$, $\lambda_{n,k}^R$ and $\lambda_{n,k}^I$ represent the real and imaginary part of $\lambda_{n,k}$ respectively.

III. Problem Formulation and Solution

A. Problem Formulation

We focus on the PM problem for CI precoding, which aims to minimize the total required transmit power at the BS, subject to the received SINR requirement of each user and the PAPR constraint on each transmit antenna. Based on our descriptions in Section II-C, we can express the CI constraints as:

$$C_1 : \mathbf{H}_n\mathbf{x}_n = \boldsymbol{\lambda}_n \bullet \mathbf{s}_n, \quad \forall n = 1, \cdots, N \tag{6}$$

$$C_2: \left(\lambda_{n,k}^R - \sqrt{\Gamma_{n,k}\sigma^2}\right)\tan\theta_t \geq \left|\lambda_{n,k}^I\right| \quad \forall n=1,\cdots,N, \quad k=1,\cdots,K \tag{7}$$

In addition to satisfying CI conditions, we expect the transmit signals to have a low PAPR. Accordingly, we enforce that the PAPR on each antenna does not exceed α, i.e.,

$$PAPR_k \leq \alpha \Leftrightarrow N\frac{\|\mathbf{z}\|_\infty^2}{\|\mathbf{z}\|_2^2} \leq \alpha \Leftrightarrow \frac{\|\mathbf{z}\|_\infty}{\|\mathbf{z}\|_2} \leq \sqrt{\frac{\alpha}{N}} = \beta$$

Therefore, considering the PAPR constraints on all transmit antennas, the PAPR constraint can be rewritten as :

$$C_3: \frac{\|\mathbf{z}_m\|_\infty}{\|\mathbf{z}_m\|_2} \leq \beta, \quad \forall m=1,\cdots,M_t \tag{8}$$

where $\mathbf{z}_m$ represents the m-th row of the transmission signal $\mathbf{Z}$. Based on the above descriptions, the considered PM problem can be mathematically formulated as:

$$\begin{aligned} P_1: \quad & \min_{\mathbf{Z}} \quad \|\mathbf{Z}\|_F^2 \\ s.t. \quad & C_0: \mathbf{X} = \mathbf{Z}\mathbf{F}_N^T \\ & C_1: \mathbf{H}_n\mathbf{x}_n = \boldsymbol{\lambda}_n \bullet \mathbf{s}_n, \quad \forall n=1,\cdots,N \\ & C_2: \left(\lambda_{n,k}^R - \sqrt{\Gamma_{n,k}\sigma^2}\right)\tan\theta_t \geq \left|\ \lambda_{n,k}^I\right| \\ & \qquad \forall n=1,\cdots,N, \quad k=1,\cdots,K \\ & C_3: \frac{\|\mathbf{z}_m\|_\infty}{\|\mathbf{z}_m\|_2} \leq \beta, \quad \forall m=1,\cdots,M_t \end{aligned} \tag{9}$$

B. Convex Transformation via Vectorization and Regularization

As can be observed, the PAPR constraint in P_1 is non-convex, and P_1 cannot be solved directly. In light of this, we firstly approximate P_1 into a SPAPR problem with a larger dimension by vectorization method.

Recalling Eq. 1 and by defining $\mathbf{s} = \mathrm{v}ec(\mathbf{S})$, $\mathbf{r} = \mathrm{v}ec(\mathbf{R})$, $\mathbf{z} = \mathrm{v}ec(\mathbf{Z})$, $\boldsymbol{\lambda} = \mathrm{v}ec(\mathbf{\Lambda})$ and $\boldsymbol{\gamma} = \mathrm{v}ec(\mathbf{\Gamma})$, the equivalent received symbol vector can be expressed as:

$$\mathbf{r} = \mathrm{d}iag\left(\mathbf{H}_1, \mathbf{H}_2, \cdots, \mathbf{H}_N\right)\left(\mathbf{F}_N \otimes \mathbf{I}_{M_t}\right)\mathbf{z} + \mathbf{n} = \mathbf{G}\mathbf{z} + \mathbf{n} \tag{10}$$

where $\mathbf{G} = \mathrm{d}iag\left(\mathbf{H}_1, \cdots, \mathbf{H}_N\right)\left(\mathbf{F}_N \otimes \mathbf{I}_{M_t}\right) \in \mathbb{C}^{KN \times M_t N}$ is the equivalent space-time channel matrix, $\mathbf{n} \in \mathbb{C}^{KN\times 1}$ is the received noise. Accordingly, P_1 can be converted to P_2 :

$$\begin{aligned} P_2: \quad & \min_{\mathbf{z}} \quad \|\mathbf{z}\|_2^2 \\ s.t. \quad & C_1: \mathbf{g}_k\mathbf{z} = \lambda_k s_k, \quad \forall k=1,\cdots,KN \\ & C_2: \left(\lambda_k^R - \sqrt{\gamma_k\sigma^2}\right)\tan\theta_t \geq \left|\lambda_k^I\right|, \quad \forall k=1,\cdots,KN \\ & C_3: \frac{\|\mathbf{z}\|_\infty}{\|\mathbf{z}\|_2} \leq \beta \end{aligned} \tag{11}$$

where the objective function is converted to the minimization of $\|\mathbf{z}\|_2^2$, $\mathbf{g}_k$ is the k-th row of $\mathbf{G}$, λ_k is the k-th row of $\boldsymbol{\lambda}$, γ_k is the k-th row of $\boldsymbol{\gamma}$ and the PAPR constraint for each antenna is reduced to a single constraint.

Since the third constraint of P_2 is still not convex, we propose to employ the regularization method by introducing a regularization term $\mu\|\mathbf{z}\|_\infty^2$ to the objective function to replace the non-convex PAPR constraint, then P_2 can be transformed into P_3:

$$\begin{aligned} P_3: \quad & \min_{\mathbf{z}} \quad \|\mathbf{z}\|_2^2 + \mu\|\mathbf{z}\|_\infty^2 \\ s.t. \quad & C_1: \mathbf{g}_k\mathbf{z} = \lambda_k s_k, \quad \forall k=1,\cdots,KN \\ & C_2: \left(\lambda_k^R - \sqrt{\gamma_k\sigma^2}\right)\tan\theta_t \geq \left|\lambda_k^I\right|, \quad \forall k=1,\cdots,KN \end{aligned} \tag{12}$$

where $\mu \geq 0$ is a weighting coefficient that compromises between power minimization and PAPR reduction. When $\mu = 0$, the problem reduces to a traditional CI-based PM problem, while when $\mu = \infty$, it means that we only pay attention to the PAPR reduction. PAPR becomes lower with the increase of the parameter μ, but meanwhile the transmission power also increases. So in practical, μ should be selected reasonably according to specific requirements.

As can be seen, P_3 is a convex optimization problem, which can be solved via off-the-shelf convex optimization tools such as CVX. In the following, we propose an iterative algorithm based on FITRA as an alternative low-complexity solution.

C. Low-Complexity Iterative Solution

Although P_3 can be directly solved, however, from the practical point of view, using CVX is not efficient especially when the problem scale is large. Therefore in this subsection, we propose an iterative algorithm to get the approximate solution of P_3 in low complexity.

Firstly, we transform P_3 into a purely real optimization problem. To be specific, we introduce:

$$\widetilde{\mathbf{z}} = \left(Re\left(\mathbf{z}\right), Im\left(\mathbf{z}\right)\right)^T, \quad \widetilde{\mathbf{\Gamma}} = \begin{pmatrix} \sigma^2\boldsymbol{\gamma} & \sigma^2\boldsymbol{\gamma} \end{pmatrix}^T$$

$$\mathbf{U} = \begin{pmatrix} \mathbf{I}_{KN\times 1} & j\mathbf{I}_{KN\times 1} \end{pmatrix}, \quad \mathbf{S}^* = \mathrm{d}iag\left(\mathbf{s}^H\right)$$

$$\widetilde{\mathbf{G}} = \begin{pmatrix} Re(\mathbf{G}) & -Im(\mathbf{G}) \\ Im(\mathbf{G}) & Re(\mathbf{G}) \end{pmatrix}, \widetilde{\mathbf{S}} = \begin{pmatrix} Re(\mathbf{S}^*) & -Im(\mathbf{S}^*) \\ Im(\mathbf{S}^*) & Re(\mathbf{S}^*) \end{pmatrix}$$

$$\widetilde{\mathbf{I}} = \begin{pmatrix} \mathbf{I}_{KN\times 1} & \mathbf{I}_{KN\times 1}/\tan\theta_t \\ \mathbf{I}_{KN\times 1} & \mathbf{I}_{KN\times 1}/\tan\theta_t \end{pmatrix}, \quad \mathbf{H}_{eq} = \widetilde{\mathbf{I}}\widetilde{\mathbf{S}}\widetilde{\mathbf{G}}$$

Based on the above, we can obtain $\mathbf{z} = \mathbf{U}\widetilde{\mathbf{z}}$. For the convenience of subsequent derivations, we relax $\|\mathbf{U}\widetilde{\mathbf{z}}\|_\infty^2$ into $\|\mathbf{U}\widetilde{\mathbf{z}}\|_\infty$, which can also realize PAPR reduction. Then P_3 can be transformed into:

$$\begin{aligned} P_4: \quad & \min_{\widetilde{\mathbf{z}}} \quad \|\widetilde{\mathbf{z}}\|_2^2 + \mu\|\mathbf{U}\widetilde{\mathbf{z}}\|_\infty \\ s.t. \quad & \mathbf{H}_{eq}\widetilde{\mathbf{z}} \succeq \widetilde{\mathbf{\Gamma}} \end{aligned} \tag{13}$$

Subsequently, we further transform the constrained optimization problem P_4 into an unconstrained optimization problem with the penalty method. By expressing the inequality constraint as $\widetilde{\mathbf{\Gamma}} - \mathbf{H}_{eq}\widetilde{\mathbf{z}} \preceq \mathbf{0}$, P_4 is transformed into P_5 shown below:

$$\begin{aligned} P_5: \min_{\widetilde{\mathbf{z}}} = & \|\widetilde{\mathbf{z}}\|_2^2 + \mu\|\mathbf{U}\widetilde{\mathbf{z}}\|_\infty \\ & + \rho\left\|max(\widetilde{\mathbf{\Gamma}} - \mathbf{H}_{eq}\widetilde{\mathbf{z}}, \mathbf{0})\right\|_2^2 \end{aligned} \tag{14}$$

where ρ is the penalty factor introduced for the inequality constraint $\widetilde{\mathbf{\Gamma}} - \mathbf{H}_{eq}\widetilde{\mathbf{z}} \preceq \mathbf{0}$. By selecting a reasonable value for ρ, solving the unconstrained optimization problem P_5 can get the approximate solution of P_4.

In the following, we propose to employ a low-complexity iterative algorithm to solve P_5. Before proceed, we firstly review the Iterative Soft-Thresholding Algorithm (ISTA) that can be used to solve the unconstrained real convex problems such as $\min_{z} F(z) = g(z) + h(z)$. Where $g(z)$ is a continuous convex function that can be non-smooth, and $h(z)$ is a continuous and smooth convex function. In each iteration of ISTA algorithm, it computes a Proximal Operator defined as:

$$Prox_{g,h}(d) = \min_{z} g(z) + \frac{\zeta}{2}\left\| z - \left(d - \frac{\bigtriangledown h(d)}{\zeta} \right) \right\|_2^2$$

where ζ is the smallest Leibniz constant of $\bigtriangledown h(z)$. Within each iteration, z is updated as: $z^{(k)} = Prox_{g,h}\left(z^{(k-1)}\right)$.

The Fast Iterative Soft-Thresholding Algorithm (FISTA) improves upon the ISTA algorithm by changing the input of each iteration to improve the convergence speed, i.e., in each iteration of the FISTA algorithm, the variable $z^{(k)}$ is updated based on a linear combination of $z^{(k-1)}$ and $z^{(k-2)}$, instead of $z^{(k-1)}$ as done in the ISTA algorithm.

Based on the above description and by defining $g(\mathbf{z}) = \|\mathbf{z}\|_\infty$, $h(\mathbf{z}) = \|\mathbf{t} - \mathbf{A}\mathbf{z}\|_2^2$, it is equivalent to using FISTA algorithm to solve the following optimization problem:

$$\min_{\mathbf{z}} \|\mathbf{z}\|_\infty + \|\mathbf{t} - \mathbf{A}\mathbf{z}\|_2^2$$

In this case, the nearest operator is actually a clipping operator, so this algorithm is also termed Fast Iterative Truncation Algorithm (FITRA), and the above problem can be effectively solved through a simple sorting algorithm.

Now consider our problem P_5, let

$$g(\mathbf{z}) = \mu\|\mathbf{U}\widetilde{\mathbf{z}}\|_\infty, h(\mathbf{z}) = \|\widetilde{\mathbf{z}}\|_2^2 + \rho\left\| max\left(\widetilde{\mathbf{\Gamma}} - \mathbf{H}_{eq}\widetilde{\mathbf{z}}, \mathbf{0}\right)\right\|_2^2$$

we can use the FITRA algorithm to solve it. However, it is noted that the penalty term is non-differentiable, so we calculate the value of $\left(\widetilde{\mathbf{\Gamma}} - \mathbf{H}_{eq}\widetilde{\mathbf{z}}\right)$ before each iteration and take out the rows of $\widetilde{\mathbf{\Gamma}}$ and $\mathbf{H}_{eq}$ that satisfy the inequality $\widetilde{\mathbf{\Gamma}} - \mathbf{H}_{eq}\widetilde{\mathbf{z}} \succeq \mathbf{0}$ to form new matrices $\widehat{\mathbf{\Gamma}}$ and $\widehat{\mathbf{H}}_{eq}$. Subsequently, we define an auxiliary vector according to the ISTA algorithm as:

$$\widetilde{\mathbf{q}} = \mathbf{d} - \frac{\bigtriangledown h(\mathbf{d})}{\zeta} = \mathbf{d} - \frac{2}{\zeta}\left(\mathbf{d} + \rho\widehat{\mathbf{H}}_{eq}^T\left(\widehat{\mathbf{H}}_{eq}\mathbf{d} - \widehat{\mathbf{\Gamma}}\right)\right)$$

where $\zeta = 2 + 2\rho\sigma_{max}^2\left(\widehat{\mathbf{H}}_{eq}\right)$ is the smallest Leibniz constant of $\bigtriangledown h(\widetilde{\mathbf{z}})$, and accordingly the Proximal Operator is

$$PROXINF(\widetilde{\mathbf{q}}) = \min_{\widetilde{z}} \quad \mu\|\mathbf{U}\widetilde{\mathbf{z}}\|_\infty + \frac{\zeta}{2}\|\widetilde{\mathbf{z}} - \widetilde{\mathbf{q}}\|_2^2$$

Moreover, since $\mathbf{z} = \mathbf{U}\widetilde{\mathbf{z}}$, $\mathbf{q} = \mathbf{U}\widetilde{\mathbf{q}}$, it can be written as $PROXINF(\mathbf{q}) = \min_{\mathbf{z}} \quad \mu\|\mathbf{z}\|_\infty + \frac{\zeta}{2}\|\mathbf{z} - \mathbf{q}\|_2^2$. It's clear now that the $PROXINF(\mathbf{q})$ operation is actually a clipping operator, i.e., $PROXINF(\mathbf{q}) = Clip_\alpha(\mathbf{q})$, and the clipping factor $\alpha = \min_{\widetilde{\alpha}} \widetilde{\alpha} + \frac{\zeta}{2}\sum\left(max(|q_i| - \widetilde{\alpha}, 0)\right)^2$ can be obtained with a simple sorting algorithm. Finally, expand $\widetilde{\mathbf{z}} = \begin{pmatrix} Re(\mathbf{z}) & Im(\mathbf{z}) \end{pmatrix}^T$ and we can get the solution of P_5. The improved FITRA algorithm is summarized in Algorithm 1 below:

Algorithm 1 Improved FITRA algorithm

Input: $\mathbf{H}_{eq}, \widetilde{\mathbf{\Gamma}}, \rho \in (0, +\infty), K_{max}$.

Initialization:

$\widetilde{\mathbf{z}}^{(0)} = \mathbf{0}$, $\mathbf{d}^{(0)} = \mathbf{0}$, $\zeta = 2 + 2\rho\sigma_{max}^2\left(\widehat{\mathbf{H}}_{eq}\right)$,

$\mathbf{U} = \begin{pmatrix} \mathbf{I} & j\mathbf{I} \end{pmatrix}$, $\varepsilon = 10^{-3}$, $\xi^{(1)} = 1$, $\tau = \rho/\zeta$

For: $k = 1, \cdots, K_{max}$

1.Obtain $\widehat{\mathbf{\Gamma}}, \widehat{\mathbf{H}}_{eq}$ by calculating $\widetilde{\mathbf{\Gamma}} - \mathbf{H}_{eq}\widetilde{\mathbf{z}}$.

2.Compute $\widetilde{\mathbf{q}} = \mathbf{d}^{(k)} - \frac{2}{\zeta}\left(\mathbf{d}^{(k)} + \rho\widehat{\mathbf{H}}_{eq}^T\left(\widehat{\mathbf{H}}_{eq}\mathbf{d}^{(k)} - \widehat{\mathbf{\Gamma}}\right)\right)$.

3.Compute $\mathbf{z}^{(k)} = PROXINF(\mathbf{U}\widetilde{\mathbf{q}}, \tau)$,

$\widetilde{\mathbf{z}}^{(k)} = \begin{pmatrix} Re\left(\mathbf{z}^{(k)}\right) & Im\left(\mathbf{z}^{(k)}\right) \end{pmatrix}^T$.

4.Update $\xi^{(k+1)} = \frac{1}{2}(1 + \sqrt{1 + 4\left|\xi^{(k)}\right|^2})$,

$\mathbf{d}^{(k+1)} = \widetilde{\mathbf{z}}^{(k)} + \frac{\xi^{(k)} - 1}{\xi^{(k+1)}}(\widetilde{\mathbf{z}}^{(k)} - \widetilde{\mathbf{z}}^{(k-1)})$.

5. Until $\frac{\left\|\widetilde{\mathbf{z}}^{(k)} - \widetilde{\mathbf{z}}^{(k-1)}\right\|}{\left\|\widetilde{\mathbf{z}}^{(k-1)}\right\|} \leq \varepsilon$.

Output: $\mathbf{z} = \mathbf{U}\widetilde{\mathbf{z}}$.

The subfunction PROXINF is shown in Algorithm 2 below:

Algorithm 2 PROXINF algorithm

Input: $\mathbf{q}, \tau \in (0, +\infty)$.

Steps:

1.Compute $\mathbf{a} = |\mathbf{q}|$.

2.Compute $\mathbf{b} = sort(\mathbf{a}, 'decent')$.

3.Compute $c_i = \frac{1}{i}\sum_{k=1}^{i}(b_k - \tau)$.

4.Compute $\alpha = max(0, max(c))$.

5.Compute $z_i = Clip_\alpha(q_i)$.

Output: $\mathbf{z}$.

IV. Simulation Results

Simulation results are presented in this section to illustrate the performance of the proposed schemes. We compare our proposed CVX-based and FITRA-based scheme with ZF approach [14], PMP approach [4], STPAPR-Min approach [10] and traditional CI approach [5]. Throughout our simulations, we consider a MISO-OFDM system with $M_t = 16$ antennas to serve $K = 12$ users, and there are $N = 16$ OFDM subcarriers. QPSK modulation is employed, and the parameters for the FITRA-based schemes are: $\mu = \infty, \rho = 10, K_{max} = 2000$.

Fig. 2 shows the total transmission power of different schemes, and we can see that the fast algorithm proposed in this work has obvious advantage in saving transmission power compared with other PAPR reduction methods.

Fig. 3 compares the PAPR of different schemes under the constraint that the received SINR of each user is no less than 0dB. It can be seen from simulation results that the proposed

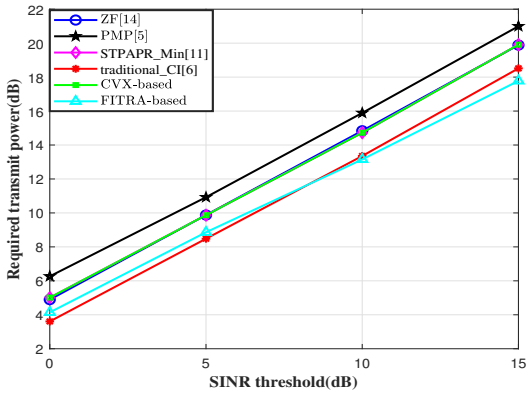

Fig. 2: Required transmit power v.s. SINR threshold, $M_t = 16$, $K = 12$, $N = 16$

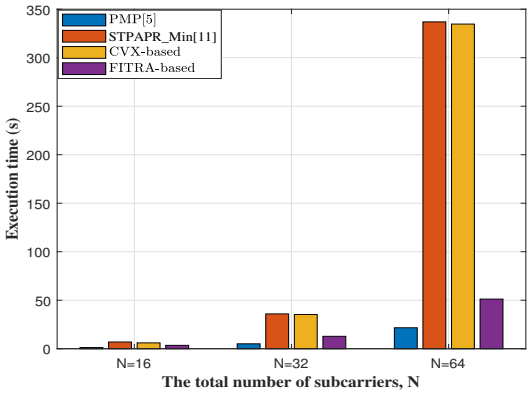

Fig. 4: Time complexity v.s. subcarrier number, $M_t = 16$, $K = 12$, $N = 16$

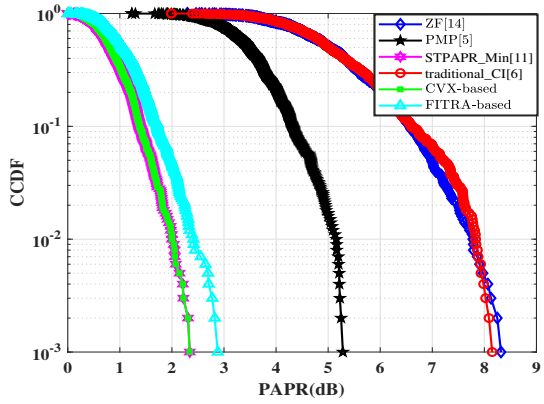

Fig. 3: CCDF of PAPR, $M_t = 16$, $K = 12$, $N = 16$

PAPR reduction scheme based on CI precoding can achieve a better PAPR performance. Specifically, our scheme achieves a PAPR of 3.0dB, which is about 5.5dB lower than that of the scheme without PAPR inhibition, and 2.7dB lower than that of PMP scheme.

The computational complexity is shown in Fig. 4 in terms of execution time. We compare the running time of our proposed algorithm with other three shemes under the constraint that the received SINR of each user is no less than 5dB. As can be seen, when the problem size is small, the average time required by all the schemes is close. But as problem size increases, the running time of the fast algorithm is much less than that of STPAPR-Min approach and CVX-based approach, which shows the efficiency of our fast algorithm.

V. Conclusion

In this letter, we propose CI-based precoding to alleviate the high PAPR issue in multi-user MISO-OFDM systems. We formulate an optimization problem to achieve low transmission power as well as low PAPR under the constructive interference constraints. Simulation results validate that our scheme achieves promising PAPR suppression and communication performance with lower complexity, compared with other existing schemes.

References

[1] K. Anoh, C. Tanriover, and B. Adebisi, "On the optimization of iterative clipping and filtering for papr reduction in ofdm systems," *IEEE Access*, vol. 5, pp. 12 004–12 013, 2017.

[2] V. Sudha, B. Anilkumar, M. Samatha, and D. S. Kumar, "A low-complexity modified slm with new phase sequences for papr reduction in ofdm system," in *2015 Annual IEEE India Conference (INDICON)*, 2015, pp. 1–5.

[3] M. Sabbaghian, Y. Kwak, and V. Tarokh, "New codes from dual bch codes with applications in low papr ofdm," *IEEE Trans. Wireless Commun*, vol. 10, no. 12, pp. 3990–3994, 2011.

[4] C. Studer and E. G. Larsson, "Par-aware large-scale multi-user mimo-ofdm downlink," *IEEE Journal on Selected Areas in Communications*, vol. 31, no. 2, pp. 303–313, 2013.

[5] A. Li and C. Masouros, "Interference exploitation precoding made practical: Optimal closed-form solutions for psk modulations," *IEEE Trans. Wireless Commun*, vol. 17, no. 11, pp. 7661–7676, 2018.

[6] A. Li, D. Spano, J. Krivochiza, S. Domouchtsidis, C. G. Tsinos, C. Masouros, S. Chatzinotas, Y. Li, B. Vucetic, and B. Ottersten, "A tutorial on interference exploitation via symbol-level precoding: Overview, state-of-the-art and future directions," *IEEE Communications Surveys Tutorials*, vol. 22, no. 2, pp. 796–839, 2020.

[7] P. V. Amadori and C. Masouros, "Constant envelope precoding by interference exploitation in phase shift keying-modulated multiuser transmission," *IEEE Trans. Wireless Commun*, vol. 16, no. 1, pp. 538–550, 2017.

[8] D. Spano, M. Alodeh, S. Chatzinotas, and B. Ottersten, "Symbol-level precoding for the nonlinear multiuser miso downlink channel," *IEEE Transactions on Signal Processing*, vol. 66, no. 5, pp. 1331–1345, 2018.

[9] D. Spano, M. Alodeh, S. Chatzinotas, J. Krause, and B. Ottersten, "Spatial papr reduction in symbol-level precoding for the multi-beam satellite downlink," in *2017 IEEE 18th International Workshop on Signal Processing Advances in Wireless Communications (SPAWC)*, 2017, pp. 1–5.

[10] D. Spano, M. Alodeh, S. Chatzinotas, and B. Ottersten, "Papr minimization through spatio-temporal symbol-level precoding for the non-linear multi-user miso channel," in *2018 IEEE International Conference on Acoustics, Speech and Signal Processing (ICASSP)*, 2018, pp. 3599–3603.

[11] ——, "Per-antenna power minimization in symbol-level precoding," in *2016 IEEE Global Communications Conference (GLOBECOM)*, 2016, pp. 1–6.

[12] F. Liu, C. Masouros, P. V. Amadori, and H. Sun, "An efficient manifold algorithm for constructive interference based constant envelope precoding," *IEEE Signal Processing Letters*, vol. 24, no. 10, pp. 1542–1546, 2017.

[13] A. Beck and M. Teboulle, "A fast iterative shrinkage-thresholding algorithm with application to wavelet-based image deblurring," in *2009 IEEE International Conference on Acoustics, Speech and Signal Processing*, 2009, pp. 693–696.

[14] M. Joham, W. Utschick, and J. Nossek, "Linear transmit processing in mimo communications systems," *IEEE Transactions on Signal Processing*, vol. 53, no. 8, pp. 2700–2712, 2005.